ADAPTATION OF A 2-D NONSEPARABLE WAVELET FILTER BANK WITH VARIABLE NUMBER OF ZERO MOMENTS

Damir Seršić, Miroslav Vrankić
Faculty of Electrical Engineering and Computing, Zagreb, Croatia

ABSTRACT

In this paper, we compare different adaptation criterions of the proposed two dimensional wavelet filter bank with a variable number of zero moments. Two-dimensional generalization of the previously reported 1-D algorithm is based on nonseparable quincunx scheme. 2-D filters were designed directly, rather then obtained from 1-D filters using pyramid scheme. Filter banks with more zero moments are better for representing smooth parts of the analyzed signal, while shorter filters are more suitable for edges and singularities. When applied to images, variable zero moment 2-D wavelets result in low ripple on edges and good concentration of wavelet coefficients in smooth parts. We discuss different adaptation algorithms based on the size of adaptation area. Chosen criterion determines decomposition properties and robustness. Results on synthetic and real images are presented.

KEY WORDS

Adaptive 2-D nonseparable wavelets, lifting scheme

1. Introduction

The number of vanishing moments of a fixed 2-D wavelet filter bank is usually chosen as a compromise between filter complexity and decomposition properties. More zero moments correspond to more regularity, which gives better description of smooth and correlated parts of the analyzed image [1][2]. However, it results in longer filters that cause spread of wavelet coefficients on sharp edges of the analyzed image. On the other hand, shorter filters are more suitable for compact representation of transients.

In this paper, we use a 2-D nonseparable quincunx wavelet filter bank that adapts the number of zero moments. Adaptation is performed on both filters in the bank at each point of decomposition. Adaptation criterion is computed from the wavelet coefficients.

In section 2 we describe the construction of proposed two-dimensional filter bank. We discuss separable and nonseparable 2-D generalizations of the one-dimensional algorithm. Sweldens 1996 [3] proposed a construction of 1-D biorthogonal wavelet filter banks based on the lifting scheme, using interpolation of samples in the time domain. Kovačević and Sweldens 2000 [4] developed a construction method for wavelet families of increasing order in arbitrary dimensions. A short review is given in paragraph 2.1. Quincunx scheme decomposes the original image into two phases (cosets). Samples from one coset are estimated from the other using 2-D interpolation functions of chosen order.

In paragraph 2.3 we explain the idea of the adjustable lifting steps.

In section 3 we discuss the adaptation criterions and results. Proposed filter bank is applied on a synthetic and a real-world image. Decomposition of synthetic image is almost optimal. Adaptation criterion computed on an area is introduced to cope with unpredictable components of the real-world signals, and the size of the area determines the robustness of the algorithm. It is shown that the entropy of the 2-D wavelet coefficients computed by adaptive filter bank is lower when compared to fixed banks.

2. Filter Bank Structure

2.1. Lifting Scheme in One Dimension

Lifting scheme enables easy construction of perfect reconstruction space-variant and non-linear filter banks. Daubechies and Sweldens [5] show that any one-dimensional two-band FIR filter bank can be factored in a set of lifting steps. Associated polyphase matrix is factored in a cascade of triangular sub-matrices. An inverse sub-matrix is obtained by a simple transposition followed by the change in sign.

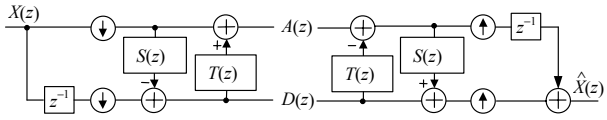

Figure 1. One-dimensional 2-channel PR filter bank factored in lifting and dual lifting steps.

$$H(z) = z^{-1} - 1 \cdot S(z^2),$$
$$L(z) = 1 + H(z) \cdot T(z^2).$$

Sweldens [3] described a lifting scheme construction of wavelet filter banks by interpolation of samples in the time domain.

2.2. Two-Dimensional Quincunx Generalization

Very often and straightforward way of generalization of the 1-D sub-band decompositions is separable (tensor product) Mallat pyramid scheme.

Although this approach is simple and widely used, it suffers from several disadvantages. Images are 2-D and thus can be better described by truly 2-D decompositions. Usual non-linear operations on wavelet coefficients (such us soft thresholding or quantization) result in artifacts that mostly lie in vertical and horizontal direction, where the human eye is especially sensitive. Instead of using Mallat pyramid scheme, we used quincunx sub-sampling method.

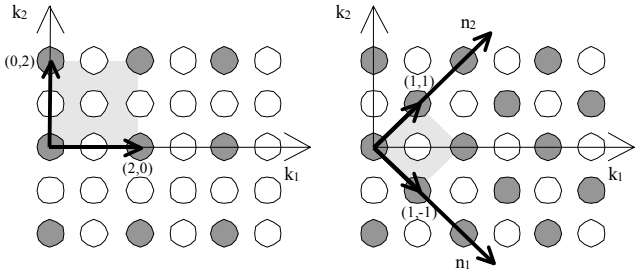

Figure 2. Separable (left) and nonseparable quincunx (right) decimation lattice. Unit cells are marked gray.

As it can be seen from **Figure 2**, nonseparable quincunx lattice has 45 degrees shift with respect to original picture coordinate axes (marked as k_1 and k_2).

Our filter structure is very similar to the one from **Figure 1** with the difference that 1-D filters are replaced with 2-D filters and simple 1-D decimation is replaced with 2-D nonseparable quincunx polyphase decomposition and decimation.

2.3. Adaptive Two-Dimensional Lifting Step

We used interpolating Neville filters to build predictor and update stage. Prediction of a X_2 coset sample is based on the interpolation from concentric rings of neighboring samples that belong to X_1 coset. Higher order of filters results in more rings included. Rings are shown in **Figure 3**.

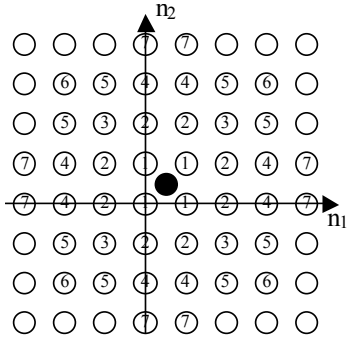

Figure 3. Quincunx lattice in the sampled domain containing X_1 coset samples. Ring numbers are marked inside circles. Black circle is the position of the predicted sample in coset X_2.

Filters are constructed using de Boor-Ron algorithm as described in Kovačević and Sweldens [4]. Coefficient values for each ring are given in **Table 1**.

Prediction filter is realized as a sum of additive components as shown in **Figure 4**. Switches p_1, p_2, p_3 and p_4 are being successively closed resulting in P_2, P_4, P_6 and P_8 filters. With m=1 prediction stage P_2 has two zero moments, m=2 gives four zero moments, etc.

N	ring 1	ring 2	ring 3	ring 4	ring 5	ring 6	ring 7	
2	1							$\times 2^{-2}$
4	10	-1						$\times 2^{-5}$
6	174	-27	2	3				$\times 2^{-9}$
8	23300	-4470	625	850	-75	9	-80	$\times 2^{-16}$

Table 1. Quincunx Neville filters coefficients. N is the number of vanishing moments.

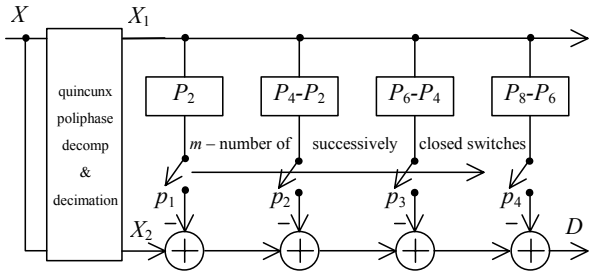

Figure 4. Adaptive lifting step (prediction stage) with 0, 2, 4, 6 or 8 zero moments of the corresponding HP filter. Switches p_1, p_2, p_3 and p_4 are being successively closed.

2.4. Adaptive Two-Dimensional Dual Lifting Step

Adaptive update step is shown in **Figure 5**. The update filter coefficients are obtained dividing appropriate prediction filter coefficients by two.

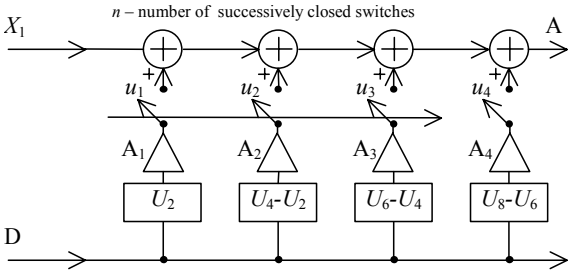

Figure 5. Adaptive dual lifting step (update stage) with 0, 2, 4, 6 or 8 zero moments of the corresponding LP filter. Switches u_1, u_2, u_3 and u_4 are being successively closed.

Switches u_1, u_2, u_3 and u_4 are also being successively closed. Number of closed switches u is marked as n.

	$m=1$	$m=2$	$m=3$	$m=4$
A_1	**1**	**1**	**1**	**1**
A_2	3/2	**1**	**1**	**1**
A_3	–	3/2	**1**	**1**
A_4	–	3/2	3/2	**1**

Table 2. A_i gain values in the update stage to obtain desired number of vanishing moments for every combination of m and n. Each column stands for chosen number of successively closed switches in the predict stage m. Every row represents a number of successively closed switches in the update stage n.

In order to obtain desired number of zero moments gains A_1, A_2, A_3 and A_4 are introduced in the update stage.

Table 2 shows the values of gains for each combination of m and n.

As it can be seen from **Table 2** if the number of zero moments of the LP filter is less or equal to the number of zero moments of the HP filter, A_i equals 1 for all $i \in \{1,2,3,4\}$. Hence, if the number of closed switches in the update filter does not exceed the number of closed switches in the prediction filter ($m \geq n$), we have "independent" lifting and dual lifting switching networks. The proposed switched structure (Figure 6) can be easily extended to similar structure enabling continuous adaptation of filter parameters (Seršić [6]).

3. Adaptation Criterions and Results

At first, we adapt the filters in order to minimize absolute error of the prediction. We analyze a synthetic image that is concatenated from 4 two-dimensional polynomials of different orders. Prediction error signal is computed as the absolute value of the wavelet coefficients D. The number of successively closed switches m is chosen to give minimum |D| at each point of decomposition. The results are shown in **Figure 7**.

We see that the adapted prediction order follows the order of polynomials. Number of closed switches is zero on discontinuities, where the filter bank degenerates to the polyphase decomposition. The decomposition is almost optimal, so the majority of adapted wavelet coefficients D are equal to zero, which was not true for fixed order wavelet decomposition.

Dual lifting step can adapt in the narrowed range $n \in (0,m)$ to provide desired number of zero moments of the low pass filter, too. We have chosen $n = m$.

background polynomial, thus producing almost zero valued wavelet coefficients.

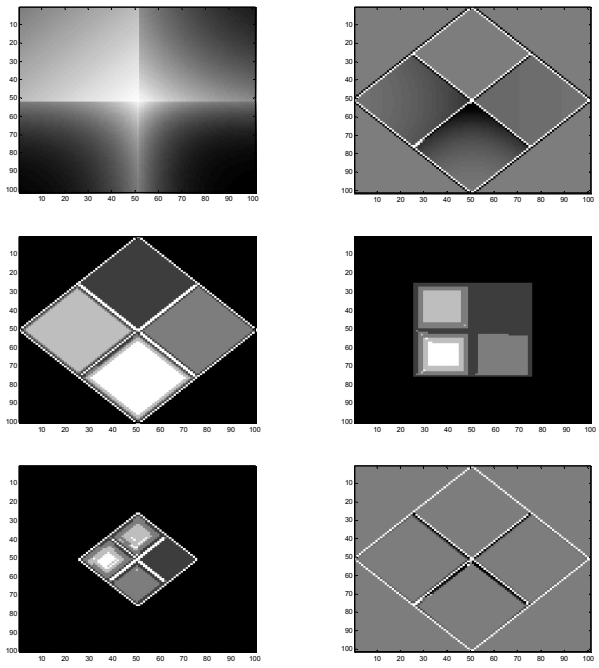

Figure 7. Top left: synthetic image composed from 4 polynomial sections of different order {1,3,5,7}. Top right: first level wavelet coefficients D computed by fixed filter bank P_2. Middle left and right, bottom left: number of closed switches m for every point of the analyzed image: levels of decomposition 1,2,3. Darkest represents $m = 0$ and brightest is for $m = 4$. Adaptation was based on minimum absolute values of wavelet coefficients at each pixel. Bottom right: first level wavelet coefficients D computed by adaptive filter bank.

Zero neighborhood adaptation criterion causes intensive variations of switches positions m (**Figure 10**, top right). Unpredictable components of the real world image make the adaptation algorithm switches very fast, making it difficult for coding.

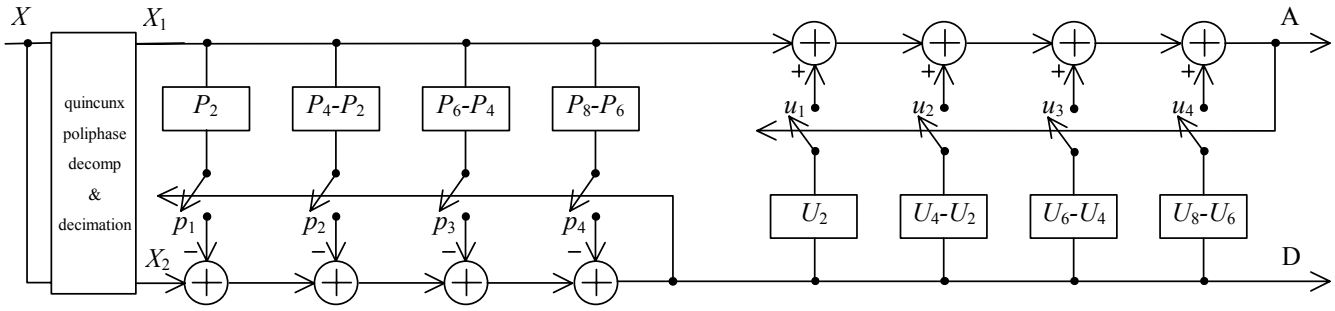

Figure 6. Adaptive wavelet filter bank. Number of successively closed update stage switches must be less or equal to the number of closed predict stage switches ($m \geq n$).

In the second example, fixed 5-level wavelet decomposition is applied to a synthetic image containing one pixel wide cross and a high order polynomial background. Then 98% of wavelet coefficients are set to zero. The reconstruction results are shown in **Figure 8**. Ringing artifacts are clearly visible in the neighborhood of cross, especially for high order wavelets.

Adaptive decomposition in 5 levels is applied to the same image, as well as the 98% zeroing. **Figure 9** shows adapted prediction orders for the first and second level of decomposition and the reconstructed image. No ringing effects are visible, due to reduction of the filter order on discontinuities. In the rest of the image filter order is sufficiently high for efficient prediction of

Sum of absolute values (p=1)			Sum of squares (p=2)		
neighbor hood K	spectrum bw of m	entropy of D	neighbor hood K	spectrum bw of m	entropy of D
0	1.25	4.85	0	1.25	4.85
1	0.75	5.31	1	0.71	5.32
2	0.54	5.35	2	0.49	5.37

Table 3. Spectrum bandwidth of switches positions m and Shannon entropy of adapted wavelet coefficients D. Entropies obtained using fixed wavelets are 5.48 and 5.35 for P_2 and P_8.

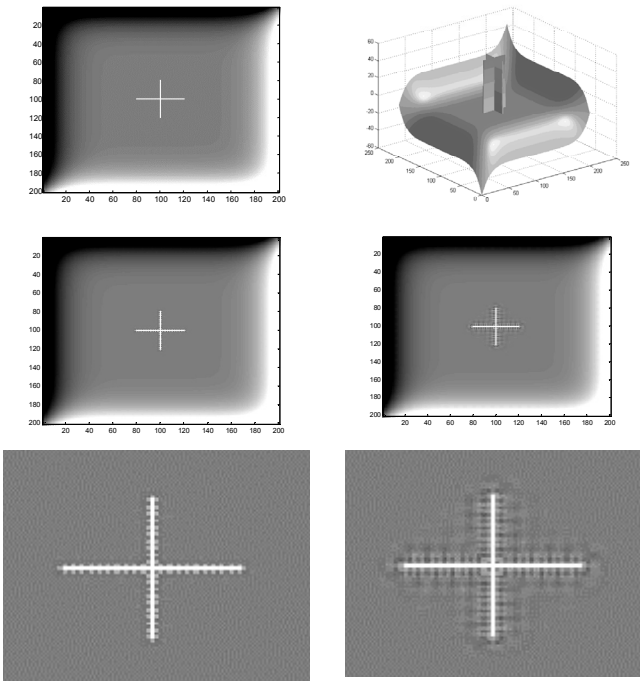

Figure 8. Top left & right: analyzed image composed from seventh order polynomial and a cross. Middle row left and right: reconstructed images obtained after fixed P_2 and P_8 five level decomposition and 98% of detail coefficients set to zero. Bottom row left and right: magnified details. Ringing artifacts are visible near cross, more for higher order predictor.

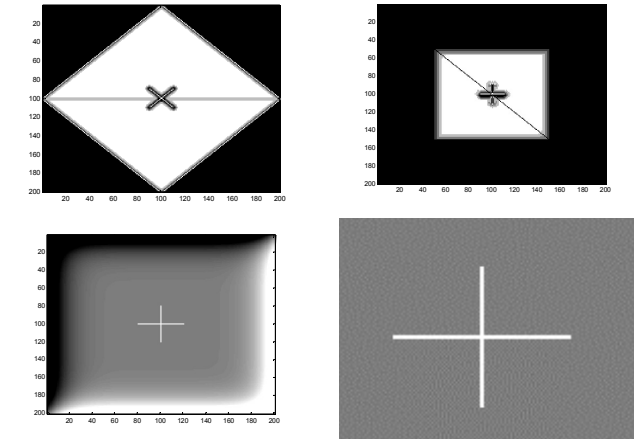

Figure 9. Top left and right: number of closed switches *m* for every point of the analyzed image for decomposition levels 1 and 2. Adaptation was based on minimum sum of absolute values. Bottom left: reconstructed image after 5 decomposition levels with 98% of adapted detail coefficients set to zero. Bottom right: magnified details. No ringing artifacts are visible.

If we use an adaptation criterion defined on a neighborhood area *K*:

$$err[k,l] = \sum_{j=l-K}^{l+K} \sum_{i=k-K}^{k+K} \left| D[i,j] \right|^p, \qquad \begin{cases} p = 1 \text{ or } 2, \\ K = 1 \text{ or } 2; \end{cases}$$

we obtain acceptable results (**Figure 10**) paid by a small increase in wavelet coefficients entropy.

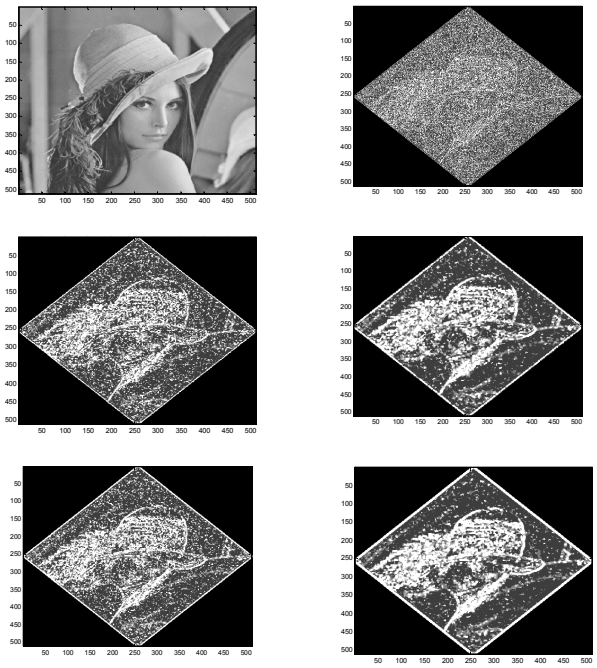

Figure 10. Top left: analyzed image. Top right: number of closed switches *m*, zero neighborhood criterion. Middle row left and right: number of closed switches *m*, criterion is minimum sum of absolute values on neighborhood 1 or 2, respectively. Bottom row: the same for minimum squares.

4. Conclusion

Proposed adaptive wavelet scheme that can change number of zero moments at each pixel has several advantages when compared to fixed wavelets. It is visible in magnified reconstructed images in **Figure 8** and **Figure 9**. Application of adaptive filter bank to the real world images results in intensive variance of switches positions that can be difficult for coding. The variance can be decreased using adaptation on the area, as shown in **Figure 10**, without significant decrease in good decomposition properties (**Table 3**). Minimum squares criterion has shown slightly better results then minimum absolute values.

5. References

[1] I. Daubechies, *Ten Lectures on Wavelets*, Society for Industrial and Appl. Math., Capital City Press, Vermont 1992

[2] D. Seršić, Wavelet filter banks with adaptive number of zero moments, *Proc. of WCC-ICSP 2000 (IEEE)*, Vol. I, pp. 325-328, Beijing, China, August 21–25, 2000

[3] W. Sweldens, The lifting scheme: A custom-design construction of biorthogonal wavelets, *Appl. Comp. Harm. Anal.*, 3(2):186-200, 1996

[4] J. Kovačević and W. Sweldens, Wavelet Families of Increasing Order in Arbitrary Dimensions, *IEEE Trans. on Image Proc*, 9(3):480-496, 2000

[5] I. Daubechies and W. Sweldens, Factoring Wavelet Transforms into Lifting Steps, *J. Fourier Anal. and Appl.*, 4(3):247-269, 1998

[6] D. Seršić, A Realization of Wavelet Filter Bank with Adaptive Filter Parameters, *Proc. of EUSIPCO 2000*, 3:1733-1736, 2000